INFLUENCE OF FLUORINE VERSUS HYDROXYL CONTENT ON THE OPTICS OF THE AMBLYGONITE- MONTEBRASITE SERIES

by

Daniel Joseph Greiner

Thesis submitted to the Faculty of the
Virginia Polytechnic Institute and State University
in partial fulfillment of the requirements for the degree of

MASTER OF SCIENCE

in

Geological Sciences

APPROVED:

F. D. Bloss, Co-Chairman

P. H. Ribbe, Co-Chairman

J. J. Brown

September, 1986
Blacksburg, Virginia

INFLUENCE OF FLUORINE VERSUS HYDROXYL CONTENT ON THE OPTICS OF THE AMBLYGONITE- MONTEBRASITE SERIES

by
Daniel Joseph Greiner

Committee Co-Chairmen: F. Donald Bloss and Paul H. Ribbe
Geological Sciences

(ABSTRACT)

For 11 crystals of the amblygonite-montebrasite series $LiAlPO_4(F,OH)$ ranging in composition from 4.0 to 91.8 mole percent fluorine with only two containing significant sodium, 2V and principal refractive indices were determined to 0.5° and 0.0005, respectively, by spindle-stage methods. If F < 60 mole percent, as is true for the vast majority of natural specimens, fluorine can usually be estimated to within 2 mole percent from the equation

$$F = -66.3 + 1.08 * 2V_z$$

as well as from similar regression equations involving the refractive indices α, β, and γ. Above 60 mole percent F, the optical properties are less sensitively (and non-linearly) related to fluorine content. Estimates of F proved feasible despite significant substitution of Na for Li. By contrast, this substitution may introduce significant errors when estimating F by methods involving lattice parameters.

Progressive substitution of (OH), a natural dipole involving a covalent bond, for the relatively non-polarizable F anion caused all three principal refractive indices to increase; γ increases more than α or ß because its corresponding principal vibration direction Z becomes sub-parallel to the O···H vector in the structure as (OH) content increases.

ACKNOWLEDGEMENTS

I would like to express my sincere appreciation to Professor F. Donald Bloss for the guidance and advice I received throughout this thesis study. I wish to also thank Professor Petr Cerny and Mrs. Iva Cerna (University of Manitoba) for kindly providing analyzed samples and for their prompt replies to my numerous questions. I am grateful to Professor Frank Hawthorne (University of Manitoba) for supplying structural data which proved invaluable. Thanks also to Professor Paul Ribbe for his critical reading of the manuscript. Mr. Mickey Gunter's and Dr. Shu-Chun Su's help with the statistical aspects of this study is greatly appreciated , as is the drafting of figures by Melody Wayne and Tom Wilson. Last , but certainly not least, I would like to thank my wife, Susan, for her unwaning support and understanding.

TABLE OF CONTENTS

LIST OF FIGURES

LIST OF TABLES

INTRODUCTION

For the amblygonite-montebrasite solid solution series

$$(\mathbf{Li,Na,Ca})^{V}(\mathbf{Al,Fe,Mg})^{VI}\mathbf{P}^{IV}\mathbf{O}_4(\mathbf{F,OH}),$$

the elements in boldface represent the primary constituents. Thus, in the common representatives of this series, less than 10% of the five-coordinated Li sites contain Na and/or Ca and less than 0.1% of the six-coordinated Al sites contain Fe and/or Mg. These specimens can consequently be regarded to represent essentially binary solid solutions between the two end members, amblygonite (amb) $LiAlPO_4F$ and montebrasite (mtb) $LiAlPO_4(OH)$. Natural members of the series range in composition from amb_0 to amb_{92}, but specimens more F-rich than amb_{65} are rare.

Members of the amblygonite-montebrasite series are triclinic and biaxial. If (-) in sign, they are called amblygonites, and if (+), montebrasites. Phillips and Griffen (1981) indicate that the optic sign changes from (+) to (-) at $amb_{\sim 35}$, but present evidence, as will be demonstrated, places the change closer to amb_{30}.

The dependence of the physical properties of the series on the dominant fluorine-hydroxyl substitution has been studied by many investigators. The usual goal has been to find one or more physical properties that will serve as reliable estimators of the F content. In such event, particularly if the physical property were quickly and precisely measurable, monitoring the F contents in members of the amblygonite-montebrasite series could permit recognition of the F-OH zoning pegmatites, where these minerals exclusively occur.

Although initiated by Bragg (1924), studies relating a crystal's optical properties to its composition and structure have been infrequent in mineralogy. A contributory factor to such neglect has been the imprecision of the available data. Thus, prior to the development of microprobe and spindle-stage techniques, a chemical analysis of a one or

two gram sample of a biaxial mineral -- itself rendered suspect because of the possible presence of admixed impurities in the sample (either as extraneous grains or inclusions in the mineral itself) -- was coupled with a principal refractive index α measured from one grain, ß from another, and γ from still a third. Moreover, the precision of their measurement, usually cited as ± 0.002 or ± 0.003, was insufficient and frequently overly optimistic. Now, however, from one and the same grain one can measure all principal refractive indices to ± 0.0005 by spindle stage, transfer the goniometer head containing the grain to an X-ray camera for such X-ray studies as desired, and, ultimately, determine this same grain's composition by microprobe analysis.

Tight relationships between optics, composition, and structure can thus be established and have led to an increasing number of recent studies (Selkregg and Bloss, 1980; Armbruster and Bloss, 1982; Su et al., 1984; Mereiter and Preisinger, 1986; Lager, 1986; to cite only a few). Combined X-ray, spindle-stage, and microprobe studies of the members of a solid-solution series have been of particular interest. As is well recognized, with the substitution of one atomic species for another in a solid-solution series, the optical properties may change, because such substitution may involve a change in atomic number and electronic shell structure, polarizability, ionic radius, valence, electronegativity, charge transfer, disposition and distances of nearest neighbors around the site of the substituent, and even the proportion of one bond type relative to another.

The amblygonite-montebrasite series was thus of interest, because it involved the replacement of a relatively non-polarizable anion, F^-, by a natural dipole, (OH^-), containing an appreciably covalent bond and capable of directional orientation in the structure. On the other hand, study of the amblygonite-montebrasite series negated one previously cited advantage. Namely, the F and (OH) contents could not be determined by microprobe analysis. In consequence, this ratio had to be determined from a sample

other than the crystal studied optically and by X-rays. On the other hand, Petr Cerny and Frank Hawthorne (University of Manitoba) generously provided crystals from very homogeneous specimens, for which fluorine and hydroxyl contents had been determined by neutron activation and gravimetric analysis, respectively.

ESTIMATION OF FLUORINE CONTENT: PREVIOUS WORK

Moss et al. (1969), using uncalibrated powder films and diffractometer tracings, determined the relationship of F content to cell parameters and to $2\theta_{131}(Cu\underline{K}\alpha_1)$ for the amblygonite- montebrasite series. Cerna et al. (1973) used diffractometer tracings of amblygonite and montebrasite powder, intermixed with quartz as an internal standard, to accomplish this. Even though the unit cell parameters showed only small variations in response to fluorine content, fluorine contents proved predictable to within 4 mole percent from $2\theta_{131}(Cu\underline{K}\alpha_1)$ values. Cerna et al. also plotted, relative to fluorine content, the peak differences $(2\theta_{hkl} - 2\theta_{101})$, where $2\theta_{hkl}$ successively represented the 121, 110, 021, 011 and 120 peaks. Again, estimates of F content to within 4 mole percent resulted. Although the method is faster than the $2\theta_{131}$ method, these peaks may overlap within several compositional ranges. Kallio (1978) utilized four uncalibrated reflections between 46° and 54°2θ $(Cu\underline{K}\alpha_1)$ to estimate fluorine contents to within 5.5 mole percent.

Fransolet and Tarte (1977) studied infrared spectra of this series and established linear relationships between fluorine content and the frequencies of both the stretching (ν_{OH}) and bending (δ_{OH}) vibrations of the (OH) molecule. ν_{OH} and δ_{OH} served to estimate fluorine content within 4 mole percent and 3 mole percent, respectively. Cerna et al. (1973) examined the applicability of specific gravity and of differential thermal analysis as determinative techniques. Neither proved useful because, as they state, "Specific gravity is too sensitive to the presence of impurities, and differential thermal behavior is too strongly dependent on the experimental setup." Loh and Wise (1976) succeeded in synthesizing ~1 μm samples at compositional intervals of 20 mole percent across the entire amblygonite-montebrasite series. Cell parameters, $2\theta_{131}$, and the gamma prime index of refraction for the (100) cleavage plane were measured and fit with

linear equations versus mole percent and weight percent fluorine.

OPTICAL CONSIDERATIONS

Research on the optical properties of the amblygonite-montebrasite series is limited. Winchell and Winchell (1951) plotted refractive index and the optical axial angle 2V versus (OH) content, using data from the literature, but the data points are widely scattered. Dubois et al. (1972) performed least-squares regressions on 2V and refractive index data measured for samples in the amb_0 to amb_{20} range. The data show considerable scatter about the trends, and these regressions indicated, for the most part, lower 2V and refractive index values than those predicted by Winchell and Winchell's graphs over the same compositional range. Cerna et al. (1973) measured the index γ' for crystals lying on the {100} cleavage and found that this index exceeded those that Winchell and Winchell had reported for γ. This underscored the need for a more accurate set of optical data for the series.

The application of spindle-stage techniques to the chemically well-characterized set of specimens assembled by Cerna et al. (Table 1) thus seemed in order. As is well known, spindle-stage techniques permit all three principal refractive indices, plus an independent value of the optic axial angle 2V, to be measured from a single grain. Cerna et al. kindly placed their set of specimens at the disposal of the writers so that crystals from the same specimens as those they had analyzed could be studied optically. As will be described next in greater detail, the resultant curves, relating fluorine mole percent to refractive index (α, ß, and γ), to optical angle 2V, and to optic orientation, permit fluorine contents to be estimated to within 2 mole percent for members of the amblygonite- montebrasite series.

EXPERIMENTAL PROCEDURES

Single crystals, preferably displaying several cleavage planes but lacking inclusions, were selected from the samples in Table 1. Each crystal was mounted on a glass fiber and affixed to a goniometer head. After transfer of this goniometer head to a Supper spindle stage mounted on a polarizing microscope, the microscope stage settings (M_S) that produced crystal extinction between crossed polars were determined at spindle-stage (S) settings of 0, 10, 20, ..., 350 degrees for sodium light. The computer program EXCALIBR (Bloss, 1981) then solved each set of extinction data and thereby calculated 2V and the settings of the spindle (S) and the microscope stage (M_S) that permitted each of the crystal's three principal refractive indices to be measured without appreciable error from misorientation.

Principle refractive indices were measured using the double variation method described by Louisnathan et al. (1978) but modified by Su et al. (1986) to include use of the computer program SOLID. This modification involves use of optical glasses, whose refractive indices are accurately known over the visible spectrum, to calibrate the method and thereby reduce systematic errors. SOLID also calculated each oil's index for the temperature and wavelength of match and then, after the crystal was studied in several oils, fit by least squares the following equations (Bloss, 1981) to the total data for the crystal:

$$n = A + B/\lambda^2 + C/\lambda^4 \qquad \text{Cauchy equation}$$

where A, B, and C are constants, and

$$y = a_0 + a_1 x \qquad \text{Linearized Sellmeier equation}$$

where $y = (n^2 - 1)^{-1}$, $a_0 = A^{-1}$, $a_1 = (\lambda_0^2 A^{-1})$, $x = \lambda^{-2}$, and where λ_0 is the central wavelength of a single absorption band (or of several closely spaced bands) in the far

Table 1. Sample descriptions and pegmatite localities.[a]
(Modified from Cerna et al. (1973).)

1.	AF-47	5,841*	Bluish water clear crystals from pegmatite vugs with quartz and cleavelandite; F content not determined [Plumbago, Newry, Maine]
2.	AF-43-2	117,775*	Grayish-white cleavage fragment [Gunnison Co., Colorado]
3.	A-22**		Brownish translucent, massive
4.	A-98**		Pale yellow translucent mass
5.	A-1**		Pale pink core of a zoned crystal (see A-2), slightly contaminated by secondary montebrasite (~5%)
6.	AF-46	105,914*	Pale bluish cleavage fragments [Karibib, South Africa]
7.	AF-55	62,576*	Colorless cleavable mass [Hebron, Maine]
8.	AF-65	14,274***	Translucent fragments with faint bluish tint [Chursdorf, Saxony]
9.	A-2**		Yellow outer rim of a zoned crystal (see A-1)
10.	A-5**		Yellow translucent, veined by A-4.
11.	AF-50	10,432*	Pale brown transparent mass [Coolgardie, West Australia]

* United States National Museum sample number
** Specimens from the Tanco pegmatite, Bernic Lake, Manitoba, Cerna et al.(1973) sample number
*** British Museum of Natural History sample number

[a]All crystals removed from these samples and studied optically were clear and contained few inclusions and showed no evidence of zoning. Crystals for AF-43, A-22, AF-50, and AF-65 each contained a few lamellae of a polysynthetic twin component. The crystal studied optically for sample AF-43 is the same crystal for which Hawthorne (pers. comm.) performed a structure analysis.

ultraviolet and where A is a constant proportional to the strength of the band(s). With the intercepts and slopes for these equations thus evaluated, the crystal's refractive index could then be calculated to within 0.0005 for wavelengths within the visible and particularly for 589.3 nm.

For six crystals, after completion of the optical work, the crystal-containing goniometer head was transferred to a precession camera. Each, unfortunately, required remounting to orient the perfect {100} cleavage, as indexed by Palache (1943) and Baur (1959), approximately perpendicular to the spindle axis and thus to the dial axis of the precession camera. After adjustments of the goniometer arcs brought $\underline{a}^*$ into precise coincidence with the dial axis, only a dial axis rotation was needed to produce centered [001]* and [010]* precession photographs.

Because the six crystals had been remounted after the initial optical study, the crystal-containing goniometer head, after removal from the precession camera, needed to be returned to the spindle stage. For three of the crystals, extinction data were again collected at 589.3 nm and solved by EXCALIBR. For these three crystals, therefore, the angular attitude of the five optic vectors relative to the $\underline{a}$, $\underline{b}$, and $\underline{c}$ crystallographic axes chosen by Palache et al. (1943) and Baur (1959) was now established at 589.3 nm. For the three other crystals, however, an optic axis was found to be nearly normal to $\underline{a}^*$ and thus nearly normal to the spindle axis when optical study was attempted. Consequently, their X-ray orientation proved to be an unfavorable orientation for spindle-stage work (Bloss, 1981). Accordingly, before collecting a new set of extinction for these crystals, the goniometer head's arcs were adjusted until the optic axis was no longer perpendicular to the spindle-stage. The resultant set of extinction data was then solved by EXCALIBR with the subroutine ARCRO invoked. ARCRO, discussed by Bloss (1981), corrects the EXCALIBR-determined positions of the five optic vectors (the two optic axes plus X, Y, and Z) back to the positions they held when

the goniometer arcs were set for the X-ray study. The optic orientation of all six crystals was now established.

DATA AND CALCULATIONS

Burri (1956) introduced the use of Euler angles to express quantitatively the optic orientation of the optical indicatrix's principal vibration axes (X, Y, and Z) relative to the crystallographic axes of a triclinic crystal. In essence, he related the intrinsically orthogonal set of axes (X, Y, and Z) to a second orthogonal set obtained by choosing: (1) a reciprocal crystallographic axis; (2) one of the two direct crystallographic axes perpendicular to it; and (3) a third axis that is perpendicular to both (1) and (2). The cleavage planes for the amblygonite-montebrasite series made it expedient to choose as the orthogonal crystallographic set the axes (1) $\underline{a}^*$; (2) $\underline{c}$; and (3) B, where B symbolizes a direction perpendicular to both $\underline{a}^*$ and $\underline{c}$. Euler angles were calculated such that if the corresponding rotations were performed, X would coincide with B, -Y with $\underline{a}^*$, and Z with $\underline{c}$ (Fig. 1).

For the specimens studied, Table 2 summarizes the values for sodium light of 2V, α, ß, and γ and the Euler angles. Moreover, since the orientation of the five optic vectors for sodium light had been determined relative to the crystallographic axes, the refractive indices exhibited by {100} cleavage flakes -- namely, γ' and α' -- could now be calculated. To do so, the angles between the γ'_{100} vibration direction and the X, Y, and Z axes (symbols: θ_x, θ_y, θ_z) were determined following a procedure discussed by Bloss (1981, p. 63). Then, using Equation 4-9a of Bloss (1981), γ'_{100} for sodium light was calculated since

$$1/(\gamma'_{100})^2 = \cos^2\theta_x/\alpha^2 + \cos^2\theta_y/\beta^2 + \cos^2\theta_z/\gamma^2 .$$

When α'_{100} was similarly calculated, its value inevitably fell within 0.0005 of that determined for α.

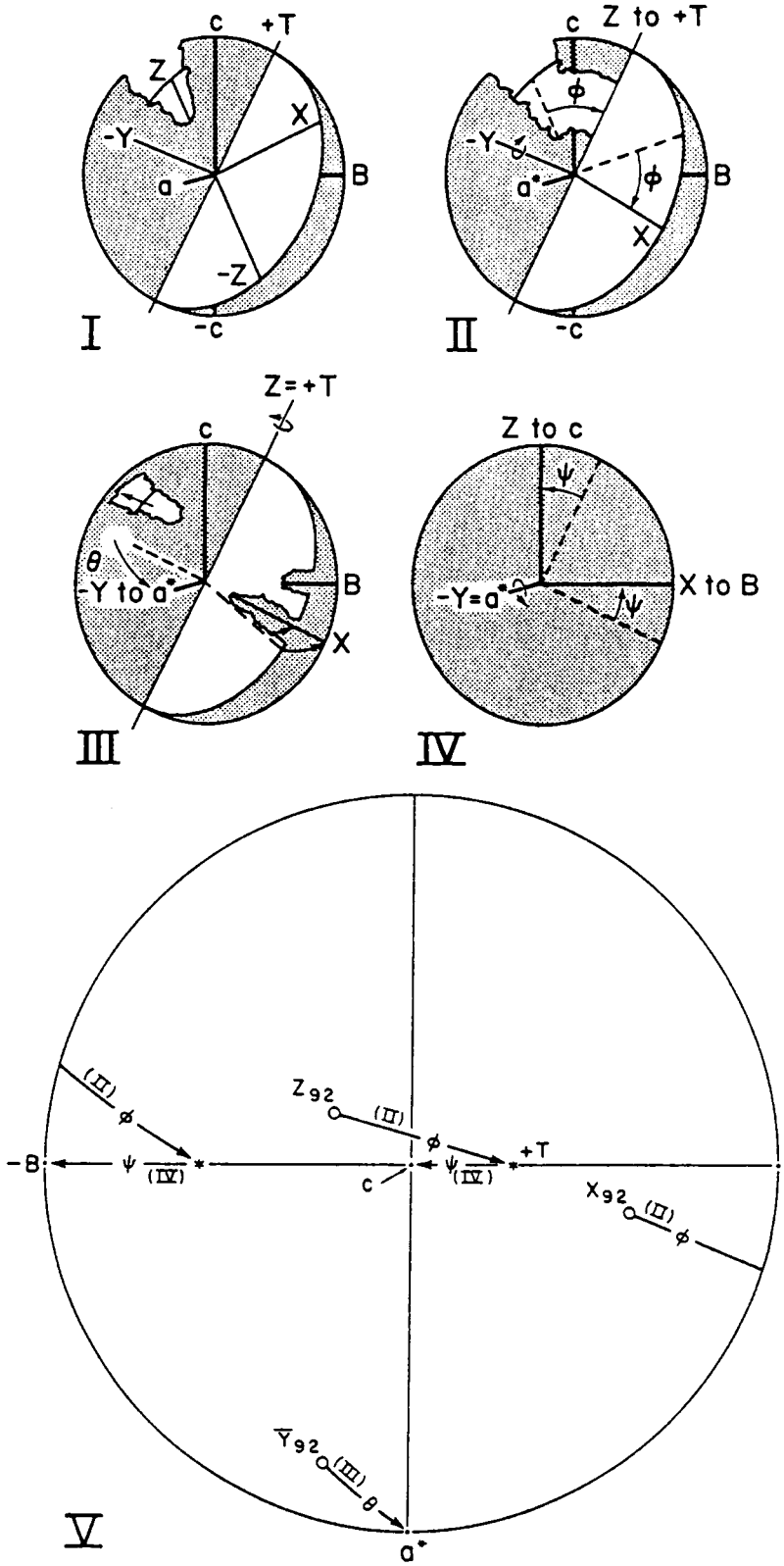
c
+T
Z
X
-Y
a
B
-Z
-c
I
c
Z to +T
Φ
-Y
a*
B
Φ
X
-c
II
Z=+T
c
θ
-Y to a*
B
X
III
Z to c
Ψ
-Y=a*
X to B
Ψ
IV
(II)
Φ
Z92
(II)
Φ
-B
Ψ
(IV)
c
Ψ
(IV)
+T
+B
X92
(II)
Φ
Y92
(III)
θ
a*
V

Table 2. Refractive indices, 2V, and Euler angles observed for sodium light.

Sample	F*	α	ß	γ	$2V_z$	γ'	ϕ	θ	ψ
1	4.0**	1.61476	1.62440	1.64589	66.27	1.64185	82.4	-26.0	77.8
2	10.8	1.61088	1.62190	1.64026	71.63	.	.	.	.
3	14.4	1.61043	1.62067	1.63800	72.82	.	.	.	.
4	26.5	1.60536	1.61533	1.62963	85.15	1.62727	86.3	-23.9	76.4
5	42.7	1.59530	1.60816	1.61784	100.76	1.61664	92.0	-20.8	77.8
6	55.3	1.58856	1.60263	1.60913	112.57	1.60871	100.5	-14.3	81.0
7	79.2	1.57923	1.59417	1.59749	125.98	1.59739	43.0	14.7	18.0
8	91.8	1.57723	1.59180	1.59560	129.47	1.59534	55.5	18.2	30.0
9	27.9	1.60052	1.61283	1.62488	92.87	.	.	.	.
10	34.8	1.59532	1.60840	1.61753	99.31	.	.	.	.
11	54.5	1.59123	1.60536	1.61273	106.98	.	.	.	.

* F = mole percent fluorine
** Calulated value, see Cerna et al. (1973)

CHEMISTRY

The crystals studied are from the same specimens as were studied by Cerna et al. (1973). These amblygonite-montebrasite crystals ranged from translucent to gem quality and overall seemed relatively homogeneous in composition throughout each single specimen (P. Cerny, pers. comm.). Microprobe analyses of these crystals disclosed magnesium and iron to be below detectable limits and calcium to be below 0.1 mole percent. Sodium proved to be below detectable limits for all samples except numbers 7 and 8 wherein it exceeded 2 percent by weight. Aluminum and phosphorous were nearly constant. This suggested that the eight crystals contained no significant substitutions other than fluorine for hydroxyl. Attempts to determine fluorine content by calculation from microprobe analyses were unsuccessful. An initial spindle-stage study of several different crystals from a given specimen yielded 2V values, as calculated by EXCALIBR, that differed by four degrees at most. Thus, it seemed valid to assume that crystals from a given specimen differed little in optical properties and composition from each other. Accordingly, the compositions given by Cerna et al. (Table 2, 1973) were accepted as valid for these crystals.

For sample 8, Moss et al. (1969) had determined its fluorine content, not by neutron activation, but from its distillate using the zirconium-Eriochrome-cyanine method of Megregian (1954). Moreover, no complementary (OH) analysis had been performed on it. Because the principal refractive indices of sample 7 exceeded those of 8 by only 0.002, the possibility arose that specimens 7 and 8 might actually have the same F contents, and that the observed differences were from analytical error and/or use of different techniques. Accordingly, counts for F were determined for microprobe analyses of specimens 1 and 3 to 7 as well as specimen 8.

For these microprobe analyses, a 10 kV, 20 nA beam was used to sample a 100

micron diameter surface. Over five cycles of 10-second-interval fluorine counts were collected and then averaged at each of 8 to 10 sites per sample. These 8 to 10 averages were themselves averaged to produce the sample average. This method appeared to best minimize the error from the time dependency of fluorine counts, while also guarding against statistical error due to the insufficient repetition of an experimental test.

Regressions were then performed on the above data for specimens 1 and 3 to 7 by taking F probe counts as the independent variable and the neutron-activation-determined fluorine contents as the dependent variable. The regression equation then obtained is

$$F \text{ (mole percent)} = 6.03 + 1.13P + 0.166P^2 \qquad R^2 = 0.98$$

where P represents the probe count for F. Inserting the P value for specimen 8 into this equation yielded a value of 91.2 mole percent F. This predicted value was in excellent agreement with 91.8 mole percent, the value calculated from the 11.8 weight percent value obtained by Moss et al. (1969).

In this paper the fluorine proportions will be expressed as mole percent fluorine ($\underline{F}$) -- that is, as $\underline{F}_A$*100 where $\underline{F}_A$ represents the atomic frequency of this element in the formula unit. $\underline{F}$ (mole percent fluorine) and $\underline{OH}$ (mole percent hydroxyl) were calculated by Cerna et al. (1973) from the weight percent values they obtained for fluorine and water. The values for $\underline{F}$ and $\underline{OH}$ were adjusted for the presence of minor Na, Ca, K, Mg, and Fe. Complete chemical analysis of sample 8 has not been performed. Accordingly, for sample 8, $\underline{F}$ was here calculated from the equation:

$$\underline{F} = 7.7845 \text{ x weight percent fluorine.}$$

This equation correctly relates mole percent to weight percent fluorine for samples wherein only the F- (OH) substitution occurs. Such a condition is not valid for AF-65, since it contains significant (>2 weight percent) Na. Still, any errors introduced by falsely assuming a lack of substitutions other than F for (OH) for these samples will be very small.

The equation:

$$\text{fluorine weight percent} = 0.12846 \times \underline{F} \ ,$$

will convert these values to weight percent fluorine for amblygonites and montebrasites in which all substitutions except (OH) for F can be considered minimal. Table 3 summarizes the content of $\underline{F}$ and $\underline{OH}$ in the specimens from which the crystals studied were drawn.

Table 3. F and OH contents.

Sample	F*	OH*	F+OH*	F_w**	H_2O+_w**	H_2O-_w**
1	4.0***	96.5	.	0.30	5.98	0.10
2	10.8	85.3	96.1	1.40	5.25	0.07
3	14.4	83.4	97.8	1.88	5.11	0.06
4	26.5	70.2	96.7	3.44	4.43	0.05
5	42.7	54.8	97.5	5.56	3.39	0.10
6	55.3	47.0	102.3	7.24	2.92	0.05
7	79.2	25.0	104.2	10.17	1.53	0.09
8	91.8	.	.	11.80	.	.
9	27.9	65.9	93.8	3.65	4.09	0.04
10	34.8	53.6	88.4	4.51	3.30	0.08
11	54.5	53.5	108.0	7.07	3.29	0.23

* In mole percent
** In weight percent
*** Calculated value; see Cerna et al. (1973)

VARIATION OF OPTICAL PROPERTIES WITH MOLE PERCENT F

Optic orientation

For the six crystals for which the optic orientation had been determined relative to the crystallographic axes chosen by Palache et al. (1943), optic orientation changed systematically as $\underline{F}$ varied from 4 to 92 (Fig. 2). Note that with increasing $\underline{F}$, the two optic axes (OA_1 and OA_2) move away from Z and approach X so that the optic sign changes from (+) and (-). For $\underline{F}$= 79 and 92, however, note that OA_1 and OA_2 are no longer moving directly toward X but are turning slightly away. Thus, $2V_x$ ceases to decrease (and $2V_z$ to increase) as rapidly with increased F when $\underline{F}$ exceeds ~ 60 percent. With increased F, one optic axis (OA_1) changes relatively little in position, whereas OA_2 changes markedly. The situation is reminiscent of another triclinic series, the plagioclase series (Reinhard, 1931), wherein as noted by Bloss (1978), one optic axis changed markedly in positions as Ca content changed, whereas the other did not.

Figure 2 shows that the optic plane remains somewhat parallel to, and rotates through, the {100} cleavage plane as fluorine content changes.

Refractive indices and 2V

Principal refractive indices (α, ß, and γ) and EXCALIBR-calculated values of $2V_z$ for sodium light were determined for specimens 1 to 11. Except for samples 1 and 8, a fluorine analysis and an independent hydroxyl analysis had been reported for each (Cerna et al., 1973). These two independent analyses were consistent for specimens 2 to 7 in that $\underline{F} + \underline{OH} \approx 100$. For specimens 9, 10, and 11, however, the sum deviated by more than 5 percent from 100 percent. Accordingly, the data for specimens 9, 10, and 11 were omitted from the calculations when regressions were performed. The following models, relating optical parameters to $\underline{F}$ (= mole percent fluorine); and indeed all

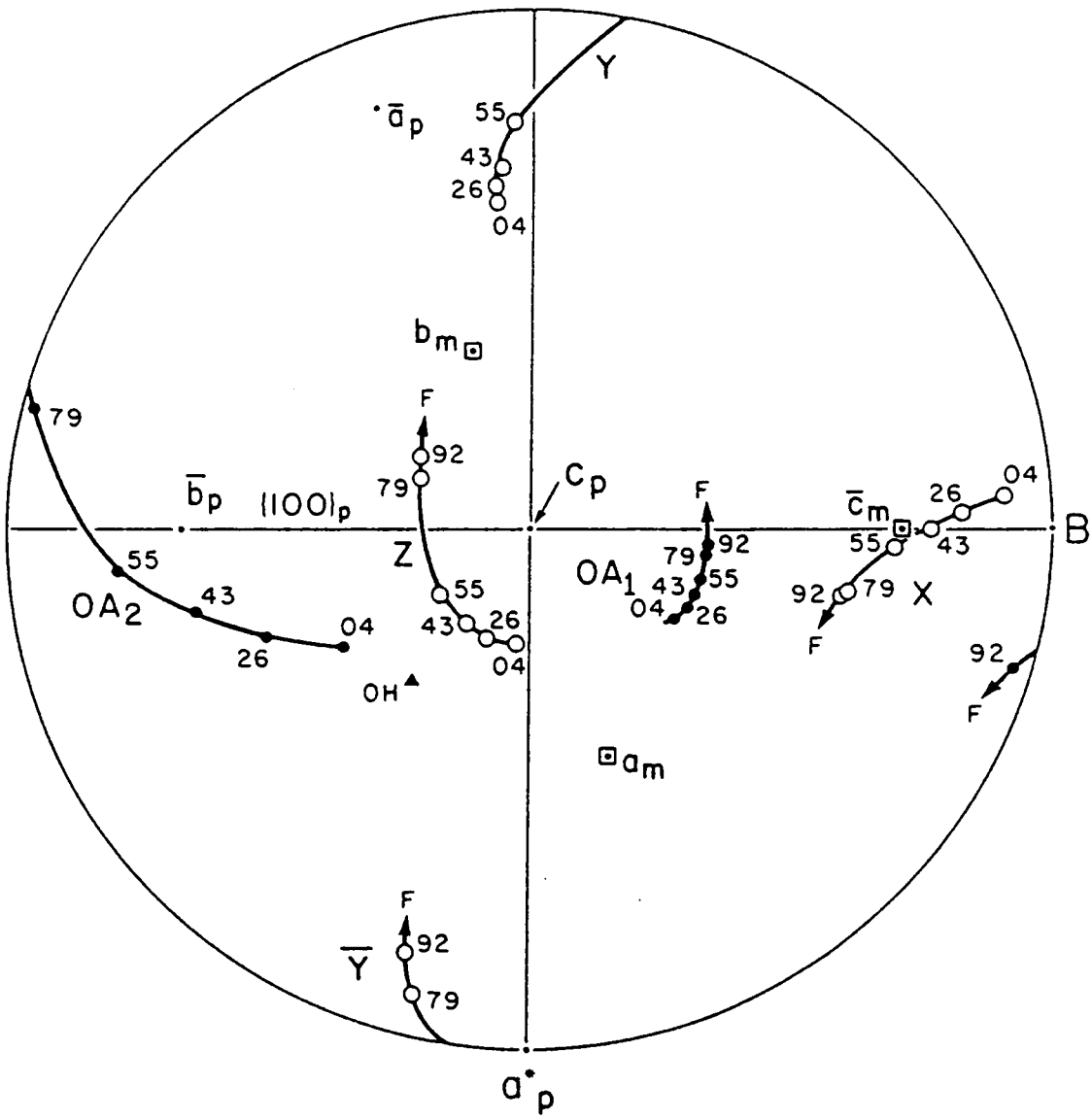
Y
$\bar{a}_p$
55
43
26
04
b_m
F
92
79
79
$\bar{b}_p$
(100)$_p$
c_p
F
$\bar{c}_m$
26
04
55
43
B
Z
55
43
26
04
OH
OA_2
OA_1
79
92
43
55
04
26
55
92
79
X
F
92
F
a_m
F
$\bar{Y}$
92
79
a^*_p

subsequent ones were derived by a combined use of the STEPWISE and RSQUARE (Cp option) procedures of the SAS Institute (1982).

		R^2
(1)	$\alpha = 1.61755(78) - 5.31(27) \times 10^{-4}\underline{F} + 1.14(33) \times 10^{-10}\underline{F}^4$	0.996
(2)	$\beta = 1.62570(11) - 3.07(11) \times 10^{-4}\underline{F} + 3.98(29) \times 10^{-6}\underline{F}^2 + 3.60(22) \times 10^{-8}\underline{F}^3$	0.999
(3)	$\gamma = 1.64884(31) - 7.50(11) \times 10^{-4}\underline{F} + 2.17(16) \times 10^{-10}\underline{F}^4$	0.999
(4)	$2V_z = 60.86(95) + 0.96(3)\,\underline{F} + 2.73(40) \times 10^{-7}\,\underline{F}^4$	0.998

These models and the data from which they were derived, along with the data for specimens 9, 10, and 11, are plotted in Figure 3. The dashed curve ($2V_{RI}$) represents $2V_z$ as calculated from the refractive index curves below it. Note that it closely conforms to the solid curve ($2V_{EX}$) representing a regression (Eq. 4) on the EXCALIBR-derived $2V_z$ values.

Although the non-linear refractive index and $2V_z$ curves in Figure 3 appear to suitably relate samples 1 through 8 to fluorine content, similar relations could not be established with fluorine taken as the dependent variable. It appears from Figure 3, however, that 2V and the principle refractive indices for the amblygonite-montebrasite series may actually vary linearly between 0 to 60 $\underline{F}$. Indeed, of regressions tested on only the optical data for specimens 1 to 6, linear models, with fluorine as the dependent variable, most aptly fit the data and are given below:

Fig. 3. Non-linear models for $2V_z$ and refractive indices versus F (mole percent fluorine). Solid refractive index curves obtain from regression Equations 1, 2, and 3. The solid curve denoted $2V_{EX}$ represents a regression (Eq. 4) of EXCALIBR-derived $2V_z$ values versus F; the dashed curve (denoted $2V_{RI}$) represents $2V_z$ as calculated from the refractive index curves below. For samples 9, 10, and 11, whose F values were uncertain, horizontal lines extend from analyzed F to 100 minus the analyzed OH value (symbolized (1-OH)). The vertical ticks indicate the values of mole percent fluorine for these samples if F plus OH is normalized to 100 percent.

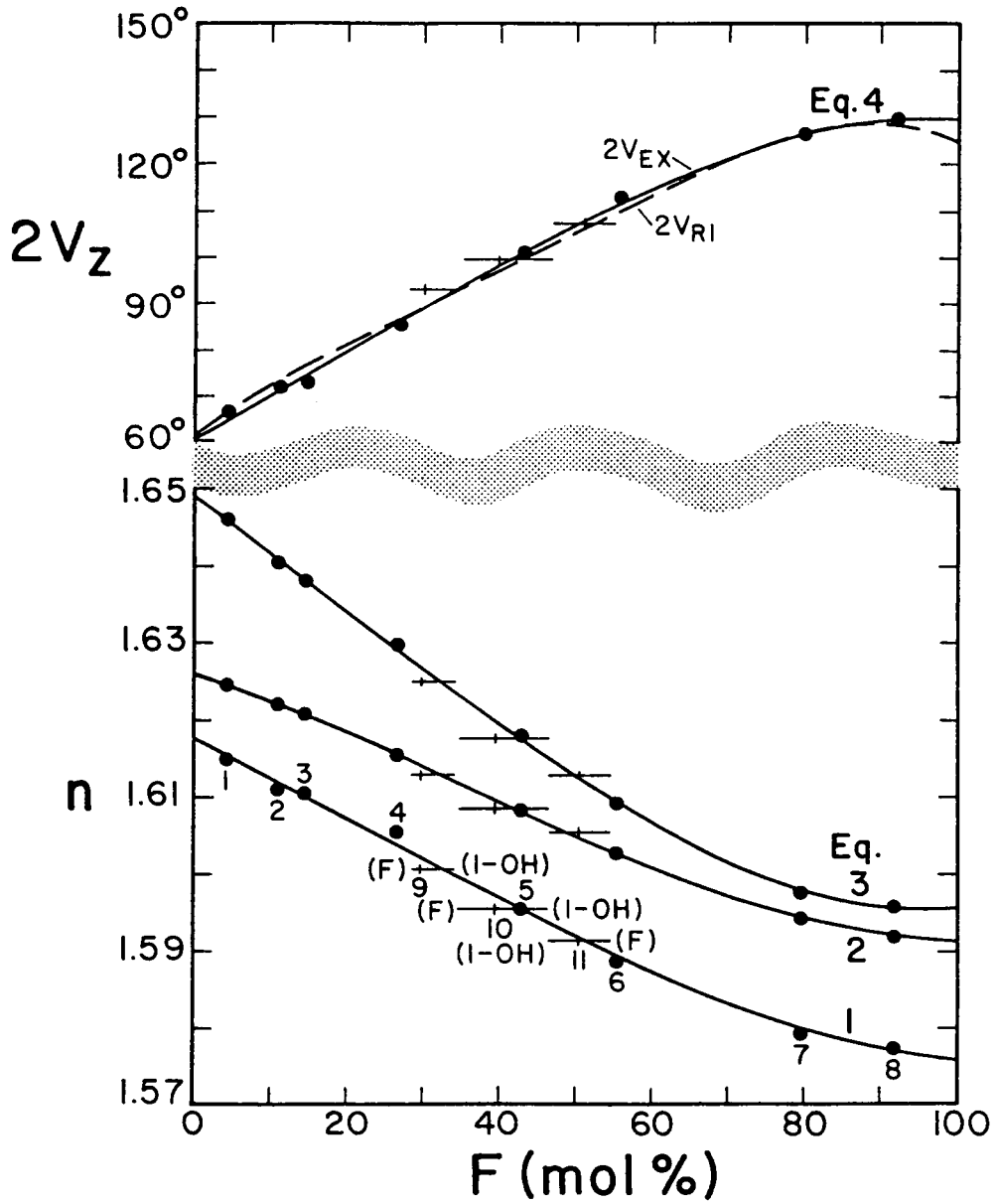
150°
120°
90°
60°
2Vz
Eq. 4
2VEX
2VRI
1.65
1.63
1.61
1.59
1.57
n
Eq. 3
2
1
(F)
(I-OH)
0
20
40
60
80
100
F (mol %)

		R^2
(5)	$\alpha = 1.61727(71) - 5.10(23) \times 10^{-4}\underline{F}$	0.996
(6)	$ß = 1.62651(20) - 4.29(6) \times 10^{-4}\underline{F}$	0.999
(7)	$\gamma = 1.64834(22) - 7.11(7) \times 10^{-4}\underline{F}$	0.999
(8)	$2V_z = 61.30(81) + 0.92(3)\,\underline{F}$	0.998

If these models were also plotted in Figure 3, their lines would closely follow along the non-linear models until $\underline{F}$ exceeded ~60 (Fig. 4). Above $\underline{F} = 60$, the linear models begin to deviate markedly from the non-linear curves of Figure 3 and do not adequately fit the 2V and refractive index data.

Upon examination of Figure 4, one might suspect that the fluorine values of samples 7 and/or 8 may actually be lower and that the linear models of refractive index are valid across the entire series. Such a scenario would require the γ and ß refractive index curves to intersect and result in the existence of a pseudo-uniaxial amblygonite at the composition wherein $\gamma = ß$. Examination of Figure 2, however, clearly shows that the migration curves of the two optic axes do not converge so as to eventually coincide with a principal direction, X in this case, as would be required of a biaxial mineral approaching uniaxiality. Instead, the two optic axes' migration curves depict $2V_z$ as steadily increasing with increased fluorine content before eventually levelling off.

Fig. 4. Linear models (dashed) compared to the non-linear models for $2V_z$ and refractive indices versus E. The linear models represent Equations 5-8.

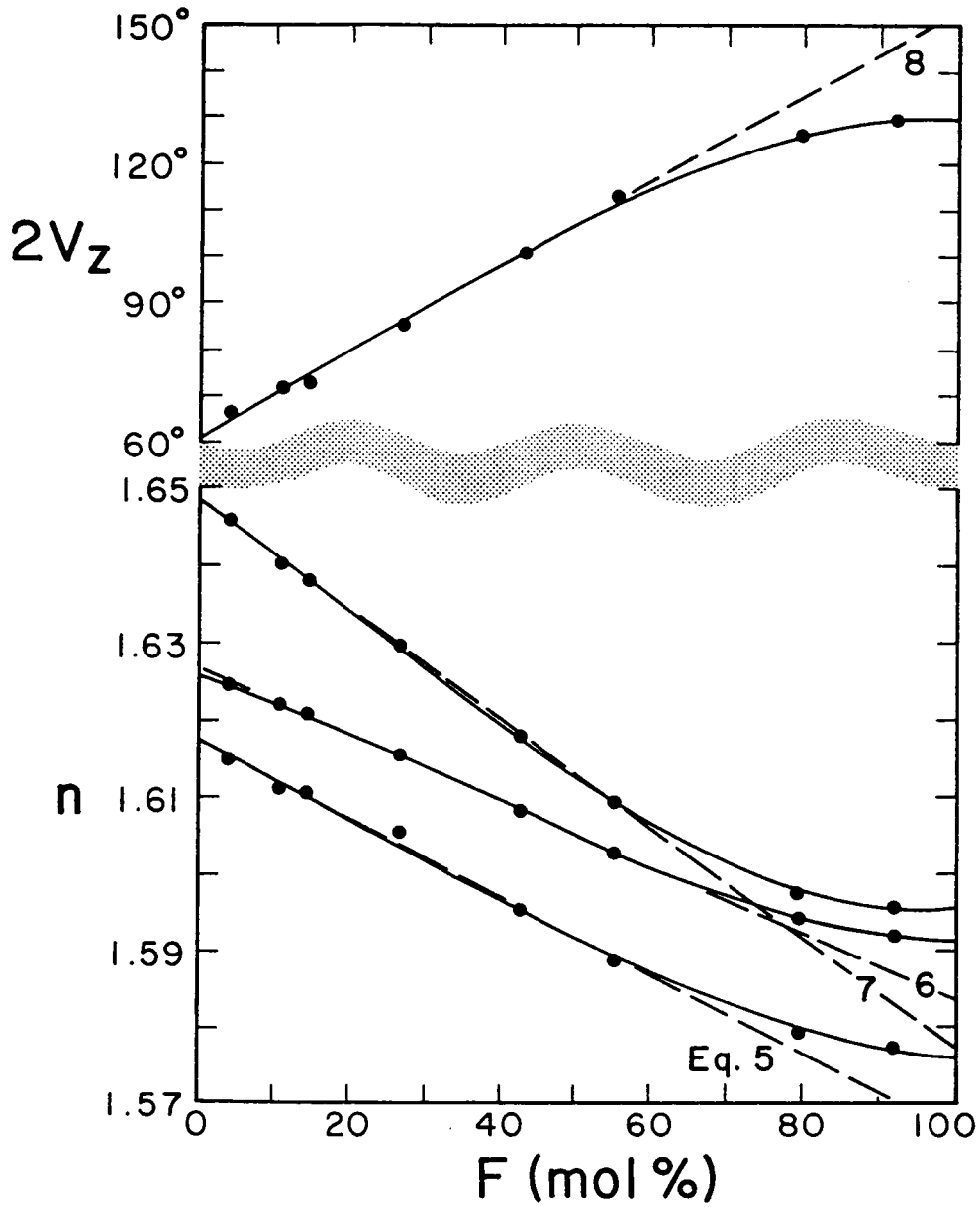
150°
120°
90°
60°
2Vz
8
1.65
1.63
1.61
1.59
1.57
n
7
6
Eq. 5
0
20
40
60
80
100
F (mol %)

PREDICTION OF MOLE PERCENT FLUORINE

Regressions, performed on the data for specimens 1 to 6 using mole percent fluorine (F) as the dependent variable, yielded the following models which are only valid for F < 60 mole percent:

		R^2
(9)	$F = 3148(139) - 1946(87)\ \alpha$	0.992
(10)	$F = 3785(56) - 2327(35)\ \beta$	0.999
(11)	$F = 2317(22) - 1405(14)\ \gamma$	0.999
(12)	$F = -66.3(2.6) + 1.08(3)\ 2V_z$	0.997
(13)	$F = 2540(12) - 1545(7)\ \gamma'$	0.999

Of these models, Equation 12 seems the most practical because: (1) $2V_z$ can be quickly measured to a fraction of a degree by using a simple detent spindle stage (Bloss, 1981) to collect extinction data for sodium light and then processing the data with EXCALIBR; and (2) accordingly, if $2V_z < \sim 115°$, fluorine should be predictable to within two mole percent. Thus, unless F exceeds 60 percent, which is rare, Equation 12 likely represents the most precise, and presumably accurate, method known yet for calculating the fluorine content of a montebrasite or amblygonite from a physical property.

Those lacking spindle stages may prefer to measure γ' for cleavage fragments lying on {100} and then use Equation 13. This will be much less satisfactory, however, and involve more work. Moreover, if γ'_{100} is only measured to ± 0.002, a 5 to 6 mole percent error in F content may result.

Table 4 compares the observed F contents -- namely, those determined directly by chemical analysis (F_{DIR}) or by hydroxyl difference (100-OH) or $F_{100\text{-}OH}$ -- with the F contents determined by inserting the measured optical parameters of samples 1-6 and

Table 4. Observed and estimated fluorine contents in mole percent for samples with $\underline{F} < 60$.

Sample	F observed from: $E_{100\text{-}OH}$*	E_{DIR}*	F predicted from: E_{α} (Eq 9)	E_{β} (Eq 10)	E_{γ} (Eq 11)	E_{2V} (Eq 12)
1*	3.5	4.0	5.1	5.0	3.5	5.5
2	14.7	10.8	12.6	10.8	11.4	11.3
3	16.6	14.4	13.5	13.6	14.5	12.6
4	29.8	26.5	23.4	26.0	26.3	25.9
5	45.2	42.7	43.0	42.7	42.9	42.8
6	53.0	55.3	56.1	55.6	55.1	55.6
9	34.1	27.9	32.8	31.8	32.9	34.3
10	46.4	34.8	42.9	42.1	43.3	41.3
11	46.5	54.5	50.9	49.2	50.0	49.6
A**	.	17.0	31.9	36.1	34.2	23.0
B***	.	45.0	59.1	.	52.4	.
C****	.	10.0	4.6	.	14.5	.

* $F_{100\text{-}OH}$ is from direct (OH) measurement, and F_{DIR} is calculated from (100-OH) for this sample.
** Haapala (1966)
*** Mookherjee (1979)
**** Gallagher (1967)

9-11 into Equations 9-12. Clearly, $2V_z$ and all three refractive indices are successful estimators of F contents between 0 and 60. $2V_z$, though, determined by spindle-stage methods, provides the most precise estimates and is much more quickly measured compared to refractive indices. Thus, it is clearly the superior monitor of F content for montebrasites and amblygonites containing F=60 or less. However, if the chemically determined F contents taken from the literature for specimens 1 to 11 were systematically high or low, the values determined from Equation 12 will also be.

For specimens 9, 10, and 11, wherein a discrepancy existed between F_{DIR} and $F_{100\text{-}OH}$, the value predicted from $2V_z$ almost coincided with $F_{100\text{-}OH}$ for specimen 9 and fell between F_{DIR} and $F_{100\text{-}OH}$ for specimens 10 and 11. Note, also, that the optical properties of sample 10 closely conform to those of sample 5.

A search of the literature disclosed three specimens (A, B and C in Table 4) for which F contents and partial optical analyses were available (Haapala, 1966; Mookerjee, 1979; Gallagher, 1967). However, significant discrepancies exist between their reported F contents and those predicted by inserting their reported optical parameters into Equation 9, 10, 11, or 12. These discrepancies may have resulted from incorrect chemical and/or optical data, or there may actually have been differences in F content between the samples examined optically and those chemically analyzed.

Cerna et al. (1973) carefully selected homogeneous material for each of the samples used in their study and, subsequently, in several other studies, including this one. Such attentive preparation of samples may have been absent in previous optical work, and thus as stated by Cerna et al.: "The differences between the analyzed and the optically studied materials in many earlier studies are the most probable explanation for the poor correlation of optics with fluorine content in Winchell and Winchell's (1951) graph." Concerning differences in F between samples analyzed chemically and samples subjected to measurement of physical properties, Cerna et al. (1973) state: "Grains and

crystals of amblygonite-montebrasite minerals frequently show primary compositional zoning and/or secondary replacement by members of the same series with different E contents."

Discrepancies between optically and chemically determined fluorine contents may also be due to the presence of fluid inclusions and daughter minerals that contain fluorine in concentrations greater or less than that of the host mineral. Fluorine contained within fluid inclusions and daughter minerals would be incorporated into the F analysis of a sample by a technique such as neutron activation. Yet, fluorine estimates based on optical properties refer only to that contained in the host mineral, assuming that the equations used for estimation were derived, as they indeed were, from a suite of samples with few inclusions. Cerna et al. (1973) reported their specimen AF-1, which contained abundant inclusions, to contain 62.7 mole percent fluorine by neutron activation (= F_{DIR}) but 73.0 percent by hydroxyl difference (= F_{100-OH}). 2V, measured for a crystal of AF-1, estimated E, by use of Equation 12, at 57.0. The sample is very cloudy and, thus, refractive indices could only be roughly estimated. Estimations from them placed E at 55 to 60. Finally, the optic orientation of AF-1 is nearly identical to that of AF-46 (E = 55.3). Thus, it appears that the host amblygonite for AF-1 contains 55 to 60 mole percent E, and that possibly F is present in a higher concentration in the fluid inclusions and daughter minerals. Microscopic examination of AF-1 revealed the presence of a cubic daughter mineral, possibly villiaumite (NaF) (R. Bodnar, pers. comm.). Thus, for samples of amblygonite and montebrasite that contain a significant amount of included material, $2V_z$ measurement is clearly superior to chemical analysis in evaluating the fluorine content of the host mineral.

Influence of Na content on F prediction

Most natural amblygonites and montebrasites contain minor Na via substitution for up to 10 mole percent Li (Dubois, 1972); thus, an evaluation as the influence of Na content on the accuracy of Equations 9-13 seems in order. The substitution of Na for Li in this series results in minor changes in density and involves ions that have very similiar polarizabilities (Pirenne and Kartheuser, 1964) and electronegativities (Pauling, 1960). This suggests that Na content should have very little effect on the relationships between optical properties and fluorine content established in this study. Indeed, the refractive indices 1.594, 1.603, and 1.615 reported by Nriagu and Moore (1984), for a sample containing ~ 56.0 mole percent Na and~ 46.5 mole percent F, agree well with the values 1.594, 1.607, and 1.615 predicted by Equations 5, 6, and 7, when $\underline{F}$ = 46.5 was inserted. Thus, unless Na content only affects the ß refractive index, which seems very unlikely, the Na content of most natural samples will not affect F predictions based on Equations 9-13.

The difference in ionic radius between Na and Li is 0.26 (Shannon and Prewitt, 1969) at minimum (considering Li as 6 coordinated). This is rather large when considering the 1.30 radius of three-coordinated F^- (Shannon and Prewitt) and the 1.34 radius of three-coordinated (OH^-) (Ribbe and Gibbs, 1971b). Thus, predictions of F content based upon subtle variations in lattice parameters will be significantly in error if the measured sample contains even minor sodium. Measurements of cell volume by Dubois et al. (1972) support this conclusion.

RELATION OF OPTICAL PROPERTIES TO STRUCTURE AND POLARIZATION

General

Cerna et al. (1973) and Hawthorne (pers. comm.) show that as (OH) content increases in the amblygonite-montebrasite series, the cell volume increases slightly, whereas the density decreases slightly. Both effects are ordinarily associated with a decrease in refractive indices. However, this effect is overwhelmed by the increase in refractive indices caused by substitution of a highly polarizable anion, (OH^-), for a relatively nonpolarizable one, F^-.

Structure

Structural analyses on the amblygonite-montebrasite series have been performed by Simonov and Belov (1958), Baur (1959), and most recently by Hawthorne (pers. comm.). Hawthorne succeeded in locating hydrogen atoms and thus, the (OH) bond vector, by difference maps. The nearly monoclinic cell employed by Hawthorne is the most useful in discussing the relations between optics and structure and will be the cell references in all figures and discussion which follow. The amblygonite-montebrasite structure, thus viewed, resembles that of titanite with Li, Al, and P replacing Ca, Ti, and Si, respectively.

Viewed along the $\underline{b}$ axis (Fig. 5), the amblygonite-montebrasite structure consists of slightly kinked chains of corner-sharing Al octahedra that run parallel to the $\underline{c}$ axis. The shared corners represent F, (OH) sites. Four membered rings, consisting of two $LiO_4(OH)$ pentrahedra alternating with two PO_4 tetrahedra, cross-link the kinked chains by sharing of (OH) and/or O with them. The C-face centering of the pseudo-monoclinic unit cell repeats these chains and rings.

Fig. 5. A portion of the structure determined by Hawthorne (pers. comm.) is here projected onto (010)* for the c-face centered nearly monoclinic unit cell he chose. The full structure results from stacking of these layers along the b-axis (by the c-face centering operation). The principal vibration axis X lies almost within this (010)* plane (see Fig. 7) and is here projected onto it (as dashed lines) for the crystals with F= 4 and 92, respectively. The shaded arrow represents how the projection position shifted as F changed from 92 to 4 in the crystals studied. This projection was derived from the positional parameters determined by Hawthorne (pers. comm.) for sample 1 (his sample AF-47).

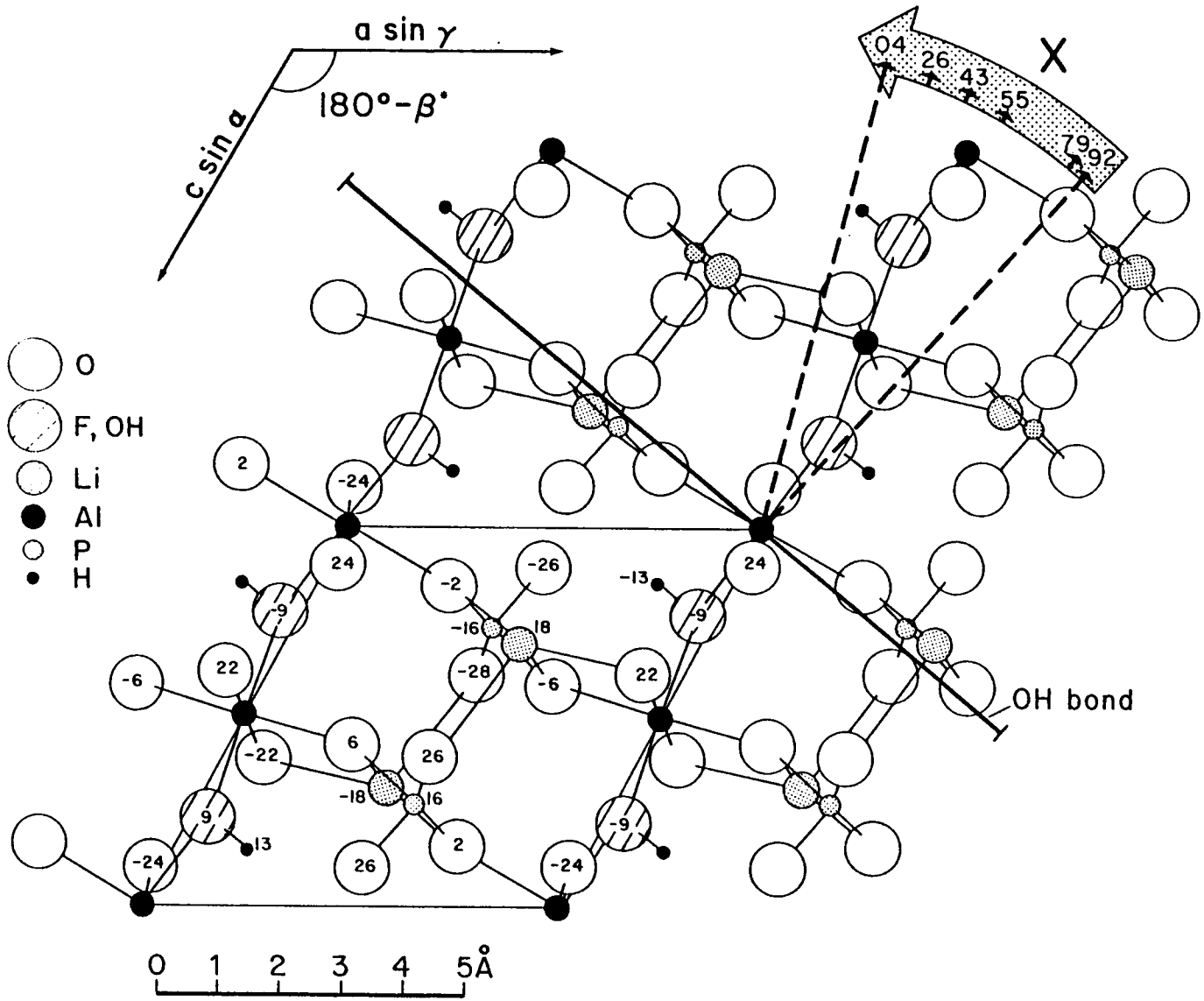
a sin γ
180°-β°
c sin α
X
04
26
43
55
79
92
O
F, OH
Li
Al
P
H
OH bond
0 1 2 3 4 5Å

Figure 6a,b offers a view of the amblygonite crystal structure viewed down the c axis. These two arrangements stack along the c axis to complete the structure.

Effect of structure and composition on optics

For hydroxyl-rich members of the amblygonite-montebrasite series, the principal vibration Z lies reasonably close to the (OH) direction (triangle, Fig. 7) that Hawthorne located. However, other structural factors must also affect the alignment of Z. If not, Z for the most (OH)-rich specimen (#1) would align closest to this (OH) direction. Moreover, as the oriented dipole (OH^-) replaces F^-, the anisotropism, as indicated by the birefringence (γ-α), increases from 0.0184 (specimen 8) to 0.0311 (specimen 1).

In Figure 3, as (OH) content increases from specimen 6 to specimen 1, γ increases at a faster rate than either ß or α because the (OH) vector is much more nearly parallel to Z than to X or Y.

When $\underline{F}$ exceeds 79, the introduction of more F into the amblygonite structure seems to yield "decreasing returns." Thus, the principal refractive indices for specimen 8 are not much smaller than those for specimen 7 (Fig. 3). Also, on the migration curves, specimens 7 and 8 plot close together. This effect led to concern that the difference in F content between 7 and 8 may only have resulted from analytical error. However, the microprobe counts for F, as already discussed, suggested that specimen 8 truly did contain around 91 or 92 mole percent F.

For the montebrasite-amblygonite series, the principal vibration direction X aligns subparallel to (010)*, whereas Y and Z align subparallel to (001)*, as Figure 7 illustrates. Accordingly, if the amblygonite structure is projected onto (010)*, this same projection approximately shows how X changes location as $\underline{F}$ changes from 92 to 4 (Fig. 5). The projection on (001)* similarly shows (Fig. 6) how Y and Z change relative to structure during this compositional change. As previously noted, Z tends to

Fig. 6. Projection onto (001)* of Hawthorne's structural data for sample 1 (= AF-47) for (a) one-half and (b) the other half of the nearly monoclinic unit cell. Principal vibration axes Y and Z, shown in Figure 7 to be subparallel to (001)*, project onto (001)* as dashed lines that shift in position as F changes from 92 to 4. For unknown reasons, directions Y and Z appear to change position relatively abruptly between F= 79 and 55. Intermediate compositions to confirm or deny this abrupt change were unavailable. The heavy line denoted "parallel to OH bond" represents the projection onto (001)* of the (OH) vector that (see Fig. 7) lies subparallel to (001)*.

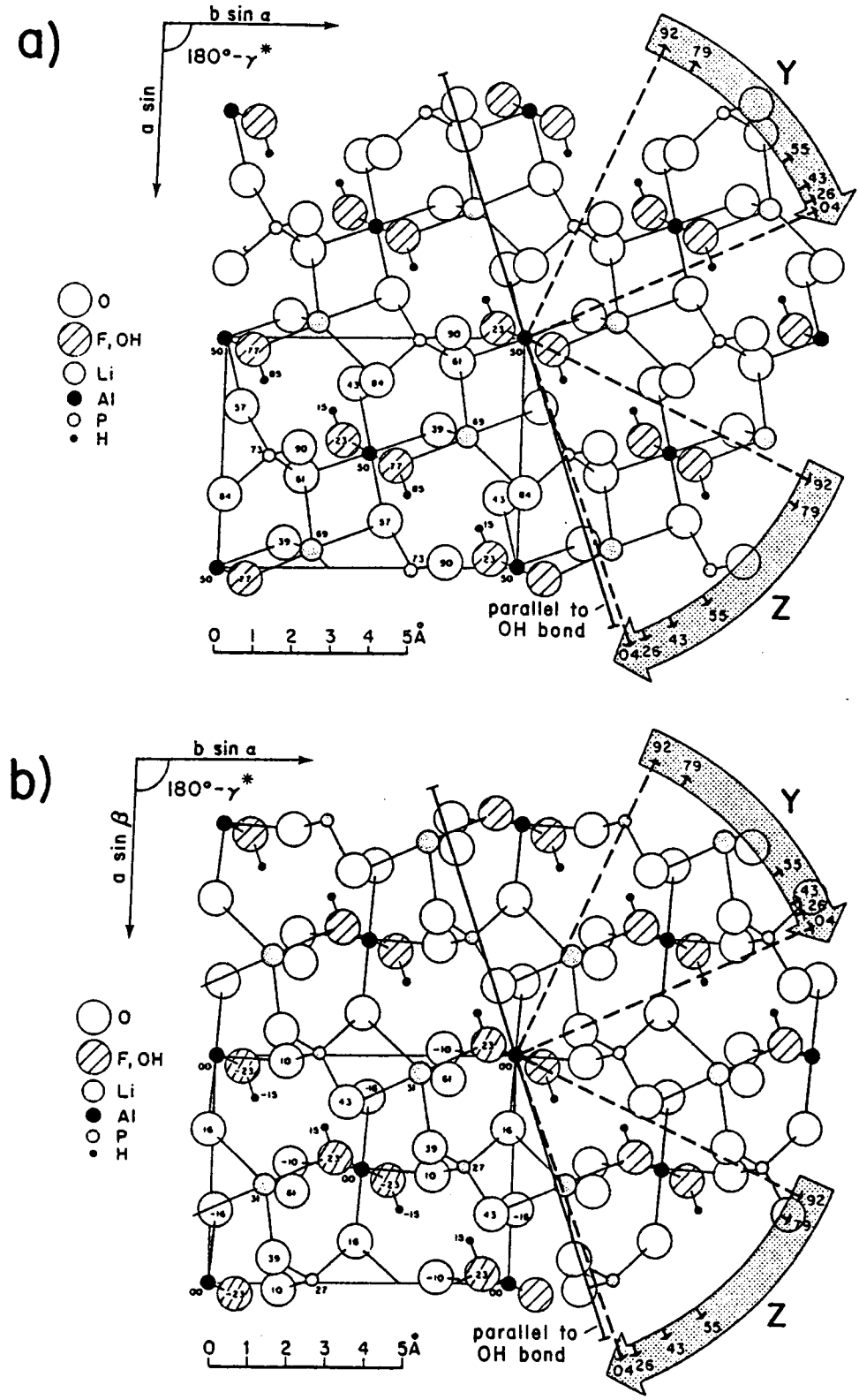
a)
b sin α
180°-γ*
a sin
O
F, OH
Li
Al
P
H
Y
Z
parallel to
OH bond
0 1 2 3 4 5Å
b)
b sin α
180°-γ*
a sin β
O
F, OH
Li
Al
P
H
Y
Z
parallel to
OH bond
0 1 2 3 4 5Å

Fig. 7. The migration curves from Figure 2 for X, Y, and Z are here stereographically projected relative to the (001)* and (010)* planes (bold great circles) for Hawthorne's nearly monoclinic unit cell. The triangles represent the (OH) vector and the averaged Al-OH bond directions as determined by Hawthorne (pers. comm.). The inset represents the angle between Z and the (OH) vector for the six crystals whose E values are listed.

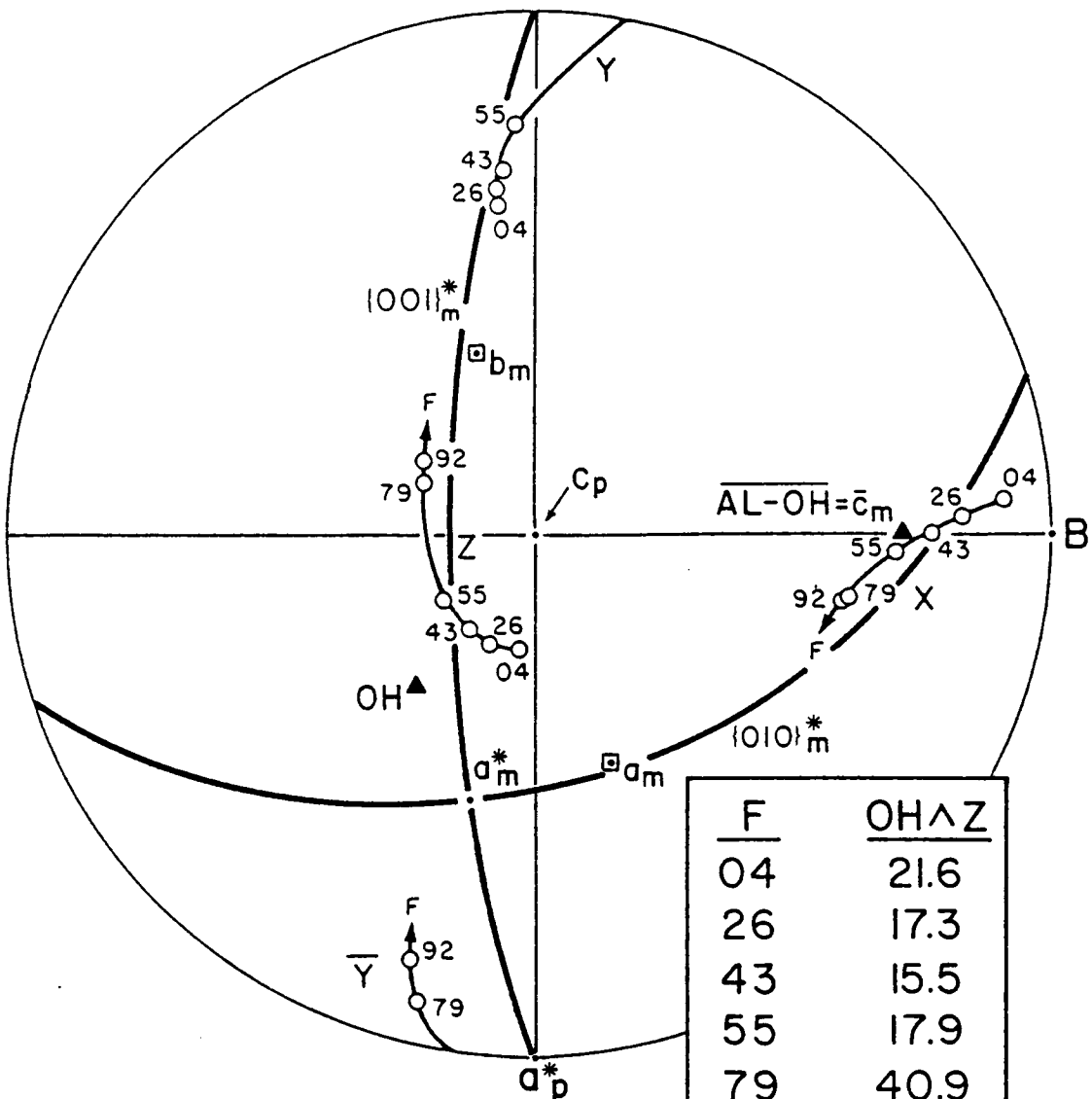

F	OH∧Z
04	21.6
26	17.3
43	15.5
55	17.9
79	40.9
92	45.8

align parallel to the (OH) vector with increasing (OH) content. Aside from the fact that X and Y must be located perpendicular to Z, no structural reasons for the precise location of X and Y were obvious.

No structural reason was arrived at to explain the relatively rapid change in orientation of the two optic axes and X, Y, and Z when $\underline{F}$ increased from 55 to 79 (Fig. 5). Also, after $\underline{F}$ exceeded 55, the curves for α, ß, γ, and 2V appeared to level off significantly (Fig. 3). Except for the "diminishing returns" conjecture, no reasons for this were apparent. Although samples 7 and 8 are the only samples in this study that have significant Na contents, it is highly unlikely that Na content is responsible for the leveling off of 2V and refractive index curves

Conclusions

1. For montebrasite-amblygonite crystals for which $\underline{F} < 60$ mole percent, their fluorine content can be estimated to ~2 mole percent from their measured values for 2V, α, ß, or γ. Results seemed relatively unaffected by sodium content.

2. Substitution of (OH^-) for F^- in the amblygonite-montebrasite structure causes the principal vibration direction Z to align subparallel to the (OH^-) vector in the structure and caused the corresponding refractive index γ to increase at a faster rate than α or ß.

REFERENCES

Armbruster, T. and Bloss, F. D. (1982) Orientation and effects of channel H_2O and CO_2 in cordierite. American Mineralogist, 67, 284-291.

Baur, W. H. (1959) Die Kristallstruktur des Edelamblygonits $LiAlPO_4(OH,F)$. Acta Crystallographica, 12, 988-994.

Bloss, F. D. (1978) The spindle stage: A turning point for optical crystallography. American Mineralogist, 63, 433-447.

Bloss, F. D. (1981) The Spindle Stage: Principles and Practice. Cambridge University Press, Cambridge and New York, 340 p.

Bragg, W.L. (1924) The refractive indices of calcite and aragonite. Proceedings of the Royal Society of London, A, 105, 370-386.

Burri, C., Parker, R. L., and Wenk, E. (1967) Die optische Orientierung der Plagioklase-Unterlagen und Diagramme zur Plagioklasebestimmung nach der Drehtische-method. Birkhauser, Basel and Stuttgart, 334 p.

Cerna, I., Cerny, P., and Ferguson, R. B. (1973) The fluorine content and some physical properties of the amblygonite-montebrasite minerals. American Mineralogist, 58, 291-301.

Dubois, J., Marchand, J., and Bourguignon, P. (1972) Donnees mineralogiques sur la serie amblygonite-montebrasite. Annales de la Societe Geologique de Belgique, 95, 285-310.

Fransolet, A. and Tarte, P. (1977) Infrared spectra of analyzed samples of the amblygonite-montebrasite series: A new rapid semi-quantitative determination of fluorine. American Mineralogist, 62, 559-564.

Gallagher, M. J. (1967) Phosphates and other minerals in pegmatites of Rhodesia and Uganda. Mineralogical Magazine, 36, 50-59.

Haapala, I. (1966) On the granitic pegmatites in the Paraseinajoke-Alavus area, South Pohjanmaa, Finland. Bull. Comm. Geol. Finlande, 224, 98 p.

Kallio, P. (1978) A new x-ray method for the estimation of fluorine content in montebrasites. American Mineralogist, 63, 1249-1251.

Lager, G. A. (1986) Prediction of refractive indices by point-dipole models (abstr.). International Mineralogical Association, 14th General Meeting, Stanford, California, U.S.A., Abstracts with Program, p. 148-149.

Loh, S. E. and Wise, W. S. (1976) Synthesis and fluorine-hydroxyl exchange in the amblygonite series. Canadian Mineralogist, 14, 357-363.

Louisnathan, S. J., Bloss, F. D., and Korda, E. J. (1978) Measurement of refractive indices and their dispersion. American Mineralogist, 63, 394-400.

Megregian, S. (1954) Rapid spectrophotometric determination of fluoride with zirconium-eriochrome cyanine R lake. Analytical Chemistry, 26, 1161-1166.

Mereiter, K. and Preisinger, A. (1986) Correlations between optical properties and crystal structures of uranyl carbonate minerals (abstr.). International Mineralogical Association, 14th General Meeting, Stanford, California, U.S.A., Abstracts with Program, p. 170.

Mookherjee, A., Basu, K., and Sanyal, S. (1979) Montebrasite and metatriplite from zoned pegmatites of Govinpal, Bastar District, M. P. Indian Journal of Earth Sciences, 6(2), 191-199.

Moss, A. A., Fejer, E. E., and Embrey, P. G. (1969) On the x-ray identification of amblygonite and montebrasite. Mineralogical Magazine, 37, 414-422.

Nriagu, J. O. and Moore, P. B. (1984) Phosphate Minerals. Springer-Verlag, Berlin, Heidelberg, New York, and Tokyo, p. 81.

Palache, C., Richmond, E., and Wolfe, C. W. (1943) On amblygonite. American Mineralogist, 28, 39-53.

Pauling, L. (1960) The Nature of the Chemical Bond, 3rd edition. Cornell University Press, Ithaca, New York.

Phillips, W. R. and Griffen, D. T. (1981) Optical Mineralogy: The Nonopaque Minerals. W. H. Freeman and Co., San Francisco, p. 77-79.

Pirenne, J. and Kartheuser, E. (1964) On the refractivity of ionic crystals. Physica, 30, 2005-2018.

Ray, A. A. (1982) SAS User's Guide: Statistics 1982 Edition. SAS Institute, Inc., Cary, North Carolina.

Reinhard, M. (1931) Universal Drehtischmethoden. Wepf, Basel, Switzerland.

Ribbe, P. H. and Gibbs, G. V. (1971b) Crystal structure of the humite minerals: III, Mg/Fe ordering and its relation to other ferromagnesian silicates. American Mineralogist, 56, 1155-1173.

Selkregg, K. R. and Bloss, F. D. (1980) Cordierites: Compositional controls of Δ, cell parameters, and optical properties. American Mineralogist, 65, 522-533.

Shannon, R. D. and Prewitt, C. T. (1969) Effective ionic radii in oxides and fluorides. Acta Crystallographica, B25, 925-946.

Simov, V. I. and Belov, N. V. (1958) The determination of the structure of amblygonite by the minimum function method. Kristallografiya, 3, 428-437.

Su, S.C. (1986) Alkali Feldspars: Ordering, Composition, and Optical Properties. Ph.D. dissertation, Virginia Polytechnic Institute and State University, Blacksburg, Virginia, p. 1-10.

Su, S. C., Bloss, F. D., Ribbe, P. H., and Stewart, D. B. (1984) Optic axial angle, a precise measure of Al,Si ordering in T_1 tetrahedral sites of K-rich alkali feldspars. American Mineralogist, 69, 440-448.

Winchell, A. N. and Winchell, H. (1951) Elements of Optical Mineralogy, Part II. Descriptions of Minerals, 4th edition. John Wiley and Sons, New York, p.

223-224.

The vita has been removed from the scanned document